Theory of pulsed NMR studies on solid D_2

T. R. J. Dinesen* and B. C. Sanctuary†
Department of Chemistry, McGill University, Montréal, Québec, Canada H3A 2K6

H. Meyer
Department of Physics, Duke University, Durham, North Carolina 27708-0305
(Received 28 December 1995)

Density matrix theory is used to calculate the response signal of both o-D_2 (with rotational angular momentum $J=0$ and nuclear spin $I=2$) and p-D_2 (with $J=I$ and $I=1$) in NMR experiments consisting of two-pulse sequences. The closed form method previously applied to the NMR ''solid echo'' of o-H_2 (with $J=I$ and $I=1$) has been extended to the deuterium system arriving at a detailed account of the dipolar interactions between like and unlike spins in a hcp lattice of concentration $X(J=1)$. The predicted solid echo amplitude for both the $I=1$ and $I=2$ contributions is expressed as a function of the mole fraction X, the pulse parameters (the angle β and relative phase φ), the time τ between the two pulses, the average spin-pair dipolar field $\overline{\delta_{jk}}$ and the average inhomogeneous field $\overline{\alpha_j}$. Agreement is good between the theoretical predictions and the experiments in which the solid echo amplitude is recorded as a function of the experimentally controllable parameters β, φ, and τ. For the $I=2$ fraction, the positions of the expected satellite echoes are determined, while failure to observe them in solid D_2 is discussed in terms of the relative magnitudes of the intramolecular coupling terms and $\overline{\alpha_j}$. [S0163-1829(96)06033-X]

I. INTRODUCTION

Solid *ortho* and *para* mixtures of the molecular hydrogens, H_2 and D_2, have been investigated over the past four decades. Much of the reason for this persistent interest is due to the cooperative orientational ordering in these crystals that is brought about by well understood anisotropic intermolecular electrostatic forces. The interaction responsible for this ordering originates from the coupling between the electric quadrupoles of non-spherical molecules, namely those with an angular momentum J different from zero. References 1–4 describe experiments and theoretical progress towards the understanding of the orientational ordering in the hydrogens, both in the regime of long-range order and in that of the gradual freezing into a ''quadrupolar glass'' state.

When cooled through their respective triple points at 14.7 and 18.6 K both H_2 and D_2 form crystals with a hcp structure. In their solid state, only the ground rotational energy levels are populated, where both o-H_2 and p-D_2 have an angular momentum $J=1$ with an electric quadrupole moment Q_e, while p-H_2 and o-D_2 have $J=0$ and $Q_e=0$. Mixtures characterized by the molar fraction $X(J=1)$ of the $J=1$ component can be prepared in any proportion.

The anisotropic electric quadrupole-quadrupole (EQQ) interaction between two isolated neighboring $J=1$ molecules tends to align these into a perpendicular ''T'' formation. The alignment in three dimensions is frustrated by the presence of both several $J=0$ and $J=1$ neighbors in the solid state. This frustration, minimized in the long-range ordered state, is most pronounced in the glassy phase. The orientational ordering that occurs as the temperature is decreased is a function of the mixture composition.[1] At temperatures below a transition line $T_\lambda(X)$, where $X_C<X<1.0$, the ordering is long-range and there is a crystalline phase change into a fcc structure (Pa_3 with interpenetrating sublattices). For the critical concentration $X_C=0.53$, the transition is at $T_\lambda=0$, while for the pure $J=1$ solids $T_\lambda=3.0$ and 4.0 K for H_2 and D_2. For mixtures with $X<X_C$, the rotational motion freezes gradually into the quadrupolar glass state, the crystalline structure remaining hcp.

There have been numerous nuclear magnetic resonance (NMR) studies of these mixtures giving abundant information on the static and dynamic properties of the spin systems. In both H_2 and D_2 the orientational ordering process is found to be very similar and an approximate scaling of the characteristic temperatures of ordering in terms of the quadrupolar interaction energy parameter Γ is obtained.[1,4] In H_2, the molecules with $J=1$ have a total nuclear spin $I=1$, while those with $J=0$ bear $I=0$. Even though the spin lattice relaxation is modulated by the relative motions of all molecules in the crystal, only the former species are capable of producing an NMR signal. In contrast, for D_2 both modifications have nuclear spins, namely the $J=1$ molecules have $I=1$ and of the $J=0$ species, 5/6 have $I=2$ while the remaining 1/6 are $I=0$. Therefore, both D_2 species produce an NMR signal.

As the temperature is decreased in the solid phase, the NMR line, initially only broadened by intermolecular dipolar interactions, becomes substantially wider below $T\approx 2$ K through the intramolecular nuclear interactions as orientational order in both H_2 and D_2 increases.[5,6] This is particularly so for the $J=1$ molecules that are directly coupled by the EQQ interaction. In contrast, orientational ordering for $J=0$ molecules is possible only through admixture of the $J=2$ state into the $J=0$ ground state via perturbation by the $J=1$ molecules,[7] and this ordering is observable for o-D_2. Therefore the line broadening in the frequency domain is appreciably smaller than that for the $J=1$ molecules and as a result the signals from both species in D_2 can be resolved.

There are nuclear dipolar interactions between *ortho* and *para* neighbors in solid D_2. Thus the NMR spectrum of D_2 is

complicated because of the presence of two distinct spin-bearing components and of their dynamic interaction. As a result the spin dynamics in D_2 are less well understood than those in the simpler H_2 system. In a strict account of the dipolar interactions, intermolecular coupling to all other spin bearing deuterons must be considered. However, since the distance between two molecules is much greater than that between two atoms in the same molecule, atomic spin states need not be accounted for *per se*, and intermolecular dipolar interactions are formally restricted to atoms with $I \neq 0$.

Two-pulse and three-pulse NMR experiments have been carried out on H_2 and were analyzed.[8,9] In particular, the response signal ''solid echo'' from the two-pulse and three-pulse sequences was studied experimentally and theoretically in some detail and could be well understood.[8] In D_2, a similar experimental program was carried out,[10,11] but at that time the theoretical formalism for the $I=2$ spins had not yet been developed. Furthermore, for the solid echo data, the analysis of the results consisted of a simple extension of the $I=1$ theory used for H_2, without proper consideration of the complete intermolecular dipolar interaction.

In these solid echo experiments on D_2 a search for the satellite echoes predicted to occur for $I=2$ systems and previously observed for D_2 embedded in an amorphous silicon matrix[12] (in which exist large crystal fields) was unsuccessful. A formal theory was needed to estimate the amplitude expected for these satellites in D_2 given the known local magnetic fields acting on the nuclei.

The purpose of our paper is to present a theory for the spin signal amplitude for both *ortho* and *para* solid D_2 for two-pulse experiments and to compare the predictions with the experimental results. In Sec. II the formal theory using a ''closed form'' method, analogous to that previously developed for $I=1$ in H_2 is presented. In Sec. III, the calculated solid echo profiles are compared with experimental data and the positions and amplitudes of the principal and satellite echoes are discussed. Section IV brings a summary.

II. THEORY

A. The single spin Hamiltonian

Here the symmetry designations of the solid hydrogens are briefly recapitulated. For the case of diatomics, if the nuclear spins have integral spin quantum number i, as in the case of D_2, then the total wave function must be symmetrical with respect to exchange of homonuclear bosons; if the spins are half-integral, as for H_2, the total wave function must be antisymmetrical to exchange of the fermions. Since both the ground state electronic and vibrational modes are always symmetrical in a diatomic molecule, the symmetry of the total wave function is determined by the product of the rotational and nuclear contributions if coupling between these four modes can be ignored. Systems with even (symmetrical) spin wave functions are designated *ortho* while those with odd (antisymmetrical) spin wave functions are designated *para*.

As mentioned in the Introduction, only the ground rotational states are populated at temperatures where the hydrogens are crystalline. This implies that the single molecule rotational wave functions are functions of the spherical harmonics $Y_{Jm}(\theta,\varphi)$. The $J=0$ state corresponds to the scalar Y_{00}, a spherically symmetrical state for which no orientational dependence is expected. This is not the case for $Y_{1m}(\theta,\varphi)$, upon which the effects of anisotropic potentials are anticipated. In the presence of intermolecular nuclear dipolar interactions, $J=1 \rightarrow J=0$ conversion takes place.[1] In D_2, where the nuclear dipole moment is much smaller than that for H_2, the $J=1 \rightarrow J=0$ conversion rate is only of the order[6] of $\Delta X = 0.5\%/24$ h for $X=0.3$ and therefore the concentration remains essentially constant during the time scale of a day's experiments.

To consider the intramolecular interactions involving the nuclear spins, the spin Hamiltonian, $\mathbf{H}_S$, for noninteracting H_2 or D_2 molecules is introduced[13]

$$\frac{\mathbf{H}_S}{\hbar} = -\alpha I_z - b_J J_z - c_{IJ}\mathbf{I}\cdot\mathbf{J} + \hbar\,\frac{\gamma^2}{i^2}\left[\frac{\mathbf{i}^{(1)}\cdot\mathbf{i}^{(2)}}{r_{12}^3} - \frac{3(\mathbf{i}^{(1)}\cdot\hat{\mathbf{n}})(\mathbf{i}^{(2)}\cdot\hat{\mathbf{n}})}{r_{12}^3}\right] + \frac{e^2 Q_n}{4i(2i-1)\hbar}\,\frac{\partial^2 V_e}{\partial z_0^2}\,[3(\mathbf{i}^{(1)}\cdot\hat{\mathbf{n}})^2 + 3(\mathbf{i}^{(2)}\cdot\hat{\mathbf{n}})^2 - i^{(1)}(i^{(1)}+1) - i^{(2)}(i^{(2)}+1)]. \tag{1}$$

By convention, the z axis is defined as lying parallel to the external magnetic field. Here I_z and J_z are the projections of the total spin $\mathbf{I}=\mathbf{i}^{(1)}+\mathbf{i}^{(2)}$ and rotational angular momentum $\mathbf{J}$ of the molecule onto this axis. The two spin operators for the nuclei in a molecule are denoted $\mathbf{i}^{(1)}$ and $\mathbf{i}^{(2)}$ and $\hat{\mathbf{n}}$ is the unit vector determining the orientation of the molecular axis. The first two terms represent the Zeeman interaction and the energy of the magnetic moment associated with molecular rotation. Spin-rotation coupling is represented by the third term. The fourth term accounts for dipole-dipole coupling of the magnetic moments $\mu=\hbar\gamma\mathbf{I}$ (where γ is the gyromagnetic ratio) of the atoms separated by the distance r_{12} while the last term, relevant only for deuterium, is the coupling of the deuteron nuclear quadrupole moment Q_n to the electric field gradient along the bond axis of the molecule $\partial^2 V_e/\partial z_0^2$.

B. Intermolecular interactions

Molecular hydrogens are the only examples of orientational quantum solids, in which the lattice molecules have a large zero point motion or a broad spatial distribution about the lattice sites and in which the angular distribution is nonlocalized, even at $T=0$. On condensation, the molecular hydrogens maintain their properties as free rotors (as suggested by low heats of melting) owing to the large rotational energies and the relatively weak anisotropic potentials in the

solid, which are dominated by the permanent electric quadrupole-quadrupole EQQ interactions between $J=1$ molecules.[1] These anisotropic energies are, in turn, much larger than the nuclear spin energies appearing in Eq. (1) so the rotational states in $\mathbf{H}_S$ can be replaced by their thermodynamic averages. At temperatures above a few mK the magnetic energies are also negligible in comparison with k_BT, in which case all components of the rotational angular momentum J_α ($\alpha=x,y,z$) have zero thermodynamic averages, $\langle J_\alpha\rangle_T=0$.[4,7,14] In other words, the rotational correlation times are much shorter than those corresponding to the nuclear spin part of $\mathbf{H}_S$ so the effect of the operators $-b_J J_z$ and $-c_{IJ}\mathbf{I}\cdot\mathbf{J}$ is effectively zero due to quenching of the orbital angular momentum.

Restricting discussion to D_2 in the crystalline state, the relevant nuclear spin Hamiltonian, including the intermolecular magnetic dipolar interaction, can be written as a sum over all molecules j in the sample

$$\frac{\mathbf{H}_{\rm tot}}{\hbar}=\sum_j\left(\begin{array}{c}-\overline{\alpha_j}I_{zj}+a_j(3i_{zj}^{(1)2}+3i_{zj}^{(2)2}-i_j^{(1)}(i_j^{(1)}+1)-i_j^{(2)}(i_j^{(2)}+1))\\ +b_j\left(i_{zj}^{(1)}i_{zj}^{(2)}-\frac{1}{4}\,i_{+j}^{(1)}i_{-j}^{(2)}-\frac{1}{4}\,i_{-j}^{(1)}i_{+j}^{(2)}\right)+I_{zj}\sum_{k\neq j}\overline{\delta_{jk}}I_{zk}\end{array}\right). \tag{2}$$

Here the first three terms are the nuclear Zeeman term and the intramolecular terms resulting from the nuclear quadrupolar and nuclear dipolar interactions with coefficients a_j and b_j. Due to the fact that the atoms in D_2 are homonuclear, the flip-flop terms in the intramolecular dipolar contribution are not quenched, resulting in a mixing of the *ortho* ($I=2$ and $I=0$) states and consequently I is not a good quantum number for o-D_2. The final term is the contribution from the intermolecular nuclear dipole-dipole interaction. Taking into consideration local field inhomogeneities, the frequency representing the average local magnetic field change is defined

$$\overline{\alpha_j}=2\mu_D(H_j-H_0)/\hbar, \tag{3}$$

where H_0 and H_j represent the external and local magnetic fields. Only the contribution of the expanded intramolecular dipole term that is secular with the Zeeman term is considered. Furthermore, both the intramolecular quadrupole and dipole coupling terms, a_j and b_j, are moderated by the degree of orientational ordering of the neighboring $J=1$ molecules in the sample. As the direct EQQ interaction between molecules with $Q_e\neq0$ tends to induce orientational alignment in the p-D_2 fraction, this molecular field also produces a perturbative alignment of the o-D_2 molecules resulting in the admixture of the $J=2$ state into the ground state,[7] owing to the existence of off-diagonal matrix elements in an otherwise vanishing Q_e. The factor $C_j(X)$ expressing this admixture has been derived by Harris[7] for the regime of long-range orientational order where $X>X_C=0.53$ and is given by $C_j(X)=(38/9)(\Gamma/B)X$ to lowest order in Γ/B, where $\Gamma/k_B=1.04$ K and the rotational energy constant $B/k_B=43$ K for D_2. For lower concentrations, where the orientational order is short range, an adequate approximation for $C_j(X)$ is obtained[15] by scaling the expression above by the local order parameter of the $J=1$ fraction in the hcp phase, $\sigma=\langle 1-(3/2)J_{zj}^2\rangle_T$, divided by the order parameter in the long-range ordered phase, $\sigma\approx1$ in which case σ is the same for each domain j. Here J_{zj}^2 is the small net projection of the angular momentum on the local symmetry axis. For these expressions of the order parameter, a cylindrical symmetry is assumed, as is reasonable for nuclei in states of well-defined angular momentum, signifying that the transverse components J_{xj}^2 and J_{yj}^2 remain quenched.[16] Hence the admixture coefficient in Eq. (5) is replaced by a temperature dependent coefficient applicable to the short-range ordered regime ''SR''.

$$C_{\rm SR}(X,T)=\frac{38}{9}\frac{\Gamma}{B}X\left\langle 1-\frac{3}{2}\,J_{zj}^2\right\rangle_T. \tag{4}$$

We then obtain expressions for the intramolecular interaction coefficients

$$a_j=\frac{5}{8}\,C_{\rm SR}(X,T)(1-3\cos^2\theta_{H,zj})d_Q, \tag{5a}$$

$$b_j=-\frac{5}{4}\,C_{\rm SR}(X,T)(1-3\cos^2\theta_{H,zj})d_M, \tag{5b}$$

where $\theta_{H,zj}$ is the angle between the magnetic field and the local symmetry axis and where[13]

$$d_Q=\frac{2e^2Q_n}{5\hbar}\,\frac{\partial^2V_e}{\partial z_0^2}=22.50\ \ {\rm kHz}$$

and

$$d_m=\frac{2\gamma_D^2\hbar}{5}\left\langle\frac{1}{r^3}\right\rangle=2.74\ \ {\rm kHz},$$

with the quantum mechanical expectation value of the interatomic distance given by $\langle 1/r^3\rangle$. For the typical concentration $X=0.3$, $C_{\rm SR}=0.02$ at $T=0.2$ K and represents the admixture of the $J=2$ rotational state into the ground state forming a symmetrical total spin state $I=2$. Of course, to consider the admixture of states in the rotational manifold of the $p-D_2$ fraction is irrelevant, so $C_{\rm SR}$ is replaced by σ for the $J=1$ molecules as regards Eq. (5) above.

For the last term of Eq. (2), that describes the intermolecular nuclear dipolar interaction for both $I=2$ and $I=1$ spins, we reiterate that a typical intermolecular distance is much greater than that between two nuclei of the same molecule. Given this, the expression for the intermolecular nuclear dipole-dipole interaction is well approximated by that representing single spins of magnitude I localized at the

centers of gravity of molecules separated by a distance R_{jk}, with the orientation of the intermolecular axis given by an angle $\theta_{R_{jk}H}$ relative to the external field. Therefore, the average intermolecular dipolar field experienced by a deuteron in molecule j due to the surrounding molecular spins k is approximated by

$$\sum_{k\neq j} \frac{\gamma_D^2\hbar}{2R_{jk}^3}(1-3\cos^2\theta_{R_{jk}H})I_{zk}=\sum_{k\neq j}\overline{\delta_{jk}}I_{zk} \tag{6}$$

and is treated as a first order perturbation of the single molecule states. Here γ_D is the gyromagnetic ratio of the deuteron. This formulation does not take into account the individual spin states of the deuterons in adjacent molecules, hence the dipolar interaction is restricted to atoms in $I\neq 0$ molecules. Given the relatively large intermolecular distances, this imposed limitation of theoretical resolution is acceptable as it merely reduces the number of intermolecular dipole coupling constants inherent to the theory.

This local field description of the dipolar interactions suggests that the dipolar field at a lattice site j is the sum of the fields arising from all other moments in the sample. Two distinct contributions to this dipolar field might then be expected, namely those due to the presence of neighboring $I=1$ and $I=2$ molecules, with respective frequencies $\overline{\delta_{j1}}$ and $\overline{\delta_{j2}}$. Of the four possible forms of $\overline{\delta_{jk}}$, the constant $\overline{\delta_{21}}$, for example, is the average intermolecular dipolar frequency experienced by a deuteron in an $I=2$ molecule due to the presence of neighboring $I=1$ spins in the lattice. In the absence of the nontrivial calculation of the lattice sum in Eq. (6) over the range in which the dipole-dipole interaction is effective,[17] it might be argued that the relative magnitudes of these fields will increase with the concentration of the spin species generating the field, i.e., $\overline{\delta_{j1}}$ should increase with X while $\overline{\delta_{j2}}$ should decrease. Since the magnitudes of these field contributions should be independent of I_{zj}, it might be considered superfluous to retain the subscript j in the $\overline{\delta_{jk}}$'s. However, this convention is maintained throughout this development in order to provide both a clearer description of the theoretical results and a means by which to gauge the validity of our suppositions regarding the intermolecular nuclear dipolar interactions, once the numerical results are presented. Based on the discussion above, we expect the following approximate relations:

$$\delta_{11}\approx\delta_{21}, \quad \delta_{12}\approx\delta_{22}. \tag{7}$$

The accuracy of these relations can be independently ascertained as the $\overline{\delta_{jk}}$'s are treated as *four independent parameters* to fit the theoretical expressions to the experimental data. Analysis of the results from both the four-parameter and the two-parameter regimen will be discussed in Sec. III A.

C. Development of the closed-form expression

A density matrix calculation of the two-pulse solid echo has been performed for the p-H_2 system.[2] Here again the intermolecular interaction is treated as a perturbation of the noninteracting Hamiltonian operating on the total spin states $|M\rangle=\Pi_j|M_j\rangle$ formed from the single molecule spin states $|M_j\rangle$. Formally, the product applies to all like spins in the sample; in practice only the aforementioned spin-pair interactions need be considered in the short-range ordered regime, reducing the problem's computational complexity. Other total spin operators may also be defined

$$I_x=\sum_j I_{xj}, \tag{8a}$$

$$I_+=\sum_j I_{+j}. \tag{8b}$$

Before application of the first rf pulse, the density matrix in the rotating frame of a system of spins I in thermal equilibrium with the lattice at temperature T is introduced

$$\rho(0)=\frac{\exp(-\mathbf{H}_{\rm tot}/k_BT)}{\mathrm{tr}\,\exp(-\mathbf{H}_{\rm tot}/k_BT)}. \tag{9}$$

Expanding Eq. (9) and applying the high field and high temperature approximations gives

$$\rho(0)\approx\frac{\hbar}{kT(2I+1)}\sum_j I_{zj}=gI_z, \tag{10}$$

where g is a constant of the system. Time evolution of the density matrix, again in the absence of a rf pulse, is determined by

$$\rho(t)=\exp\left(-\frac{i}{\hbar}\mathbf{H}_{\rm tot}t\right)\rho(0)\exp\left(\frac{i}{\hbar}\mathbf{H}_{\rm tot}t\right). \tag{11}$$

When the pulse width is much shorter than the characteristic time for free induction decay (a ''hard'' pulse) the influence of the rf field can be represented by a unitary transformation defined by the rotation operator $\mathbf{R}$. Using the phase convention and the definition of the Euler angles (α,β,γ) given by Edmonds,[18] as well as the components of the standard angular momentum operator $\mathbf{L}^2=L_x^2+L_y^2+L_z^2$ and cyclic permutations of the commutation relation $[L_x,L_y]_-=i\hbar L_z$, the effect of hard pulses is determined by the Wigner rotation matrix

$$\begin{aligned}\mathbf{R}^L_{nm}(\alpha,\beta,\gamma)&=\exp\left(\frac{i}{\hbar}\alpha L_z\right)\exp\left(\frac{i}{\hbar}\beta L_y\right)\exp\left(\frac{i}{\hbar}\gamma L_z\right)\\&=a^l_{nm}(\beta)\exp(i(m-n)\varphi)\end{aligned} \tag{12}$$

expressed in terms of the pulse angle β and phase φ. By convention, a pulse with $\varphi=0$ is denoted x and one with $\varphi=\pi/2$ is denoted y. In this investigation, it is always the case that the first pulse has $\beta=\pi/2$ and $\varphi=0$ and therefore this is a $(\pi/2)_x$ pulse. Subsequent to such a pulse, transformation of Eq. (9) gives

$$\rho(0^+)=\mathbf{R}^\dagger\rho(0)\mathbf{R}=gI_x. \tag{13}$$

The remainder of the pulse sequence involves a period of evolution as per Eq. (11) of duration τ, followed by a second hard pulse $\mathbf{R}_2(\beta,\varphi)$ of arbitrary angle and phase with a final evolution period t, in which the solid echo is collected. The evolution of the density matrix in this time interval is given by

$$\rho(t)=\exp\left(-\frac{i}{\hbar}\,\mathbf{H}_{\rm tot}t\right)\mathbf{R}_2^{\dagger}\exp\left(-\frac{i}{\hbar}\,\mathbf{H}_{\rm tot}\tau\right)$$
$$\times(gI_X)\exp\left(\frac{i}{\hbar}\,\mathbf{H}_{\rm tot}\tau\right)\mathbf{R}_2\,\exp\left(\frac{i}{\hbar}\,\mathbf{H}_{\rm tot}t\right). \quad (14)$$

The expectation value of an operator is determined by the quantum mechanical trace and by the time evolution of the density matrix

$$\langle\mathbf{A}(t)\rangle=\mathrm{tr}(\rho(t)\mathbf{A}). \quad (15)$$

Then, the detectable transverse signal at time t after the second pulse is

$$S_+(t)=\frac{\mathrm{tr}(\rho(t)I_+)}{\mathrm{tr}(\rho(0^+)I_X)}=\frac{\mathrm{tr}(\rho(t)I_+)}{\mathrm{tr}(gI_X^2)}, \quad (16)$$

for which

$$\mathrm{tr}(gI_x^2)=g\,\frac{I(I+1)}{3}\,N(2I+1)^N$$

amounts to a normalization over the sample where N is the number of *ortho* or *para* deuterium molecules. It should be noted at this time that, in practice, this normalization is treated as an arbitrary amplitude correction, for reasons to be discussed shortly.

In evaluating the trace in the numerator of Eq. (16), a closed form method is used to explicitly calculate the independent contributions to the echo by evaluating the nonzero matrix elements subject to the selection rules to be discussed. To begin, Eq. (14) is expanded making use of the completeness relation

$$\sum_M |M\rangle\langle M|=1, \quad (17)$$

so that

$$S_+(t)=\frac{1}{\mathrm{tr}(gI_x^2)}\sum_j\left(\left\langle M\left|\exp\left(-\frac{i}{\hbar}\,\mathbf{H}_{\rm tot}t\right)\mathbf{R}_2^{\dagger}\right|M'\right\rangle\left\langle M'\left|\exp\left(-\frac{i}{\hbar}\,\mathbf{H}_{\rm tot}\tau\right)gI_X\right|M''\right\rangle\left\langle M''\left|\exp\left(\frac{i}{\hbar}\,\mathbf{H}_{\rm tot}\,\tau\right)\mathbf{R}_2\right|M'''\right\rangle\right.$$
$$\left.\times\left\langle M'''\left|\exp\left(\frac{i}{\hbar}\,\mathbf{H}_{\rm tot}t\right)I_+\right|M\right\rangle\right). \quad (18)$$

Again, it is anticipated that the intermolecular dipolar interaction may be effectively treated as a sum of pairwise interactions in the short-range ordered hcp phase of D_2. As mentioned previously, the pair eigenstates and the rotation matrices are defined as

$$|M_jM_k\rangle=|M_j\rangle|M_k\rangle, \quad (19)$$

$$\mathbf{R}_{jk}=\mathbf{R}_j\mathbf{R}_k, \quad (20)$$

resulting in

$$S_+(t)=\frac{1}{\mathrm{tr}(gI_x^2)}\sum_{M_jM_j'M_j''M_j'''}\;\sum_{M_kM_k'M_k''M_k'''}\langle M_jM_k|\mathbf{R}_{2jk}^{\dagger}|M_j'M_k'\rangle\langle M_j'M_k'|I_{xj}\mathbf{E}_k|M_j''M_k''\rangle\langle M_j''M_k''|\mathbf{R}_{2jk}|M_j'''M_k'''\rangle$$
$$\times\langle M_j'''M_k'''|I_{+k}\mathbf{E}_k|M_jM_k\rangle\exp[i([-\overline{\alpha_j}(M_j'''-M_j)+(E_{b_j}'''-E_{b_j})+(E_{a_j}'''-E_{a_j})+\overline{\delta_{jk}}(M_j'''M_k'''-M_jM_k)]t)]$$
$$\times\exp[i([-\overline{\alpha_j}(M_j''-M_j')+(E_{b_j}''-E_{b_j}')+(E_{a_j}''-E_{a_j}')+\overline{\delta_{jk}}(M_j''M_k''-M_j'M_k')]\tau)]. \quad (21)$$

$\Sigma_{M_jM_j'M_j''M_j'''}$ and $\Sigma_{M_kM_k'M_k''M_k'''}$ are sums over the molecular spin states of molecules j and k. $\mathbf{E}_k$ is the unit matrix operating on spins k and E_{b_j} and E_{a_j} are the intramolecular dipole and quadrupole eigenvalues.

For $I=2$, the nonzero matrix elements of I_x generate the selection rules:

$$M_j'=\pm2,\quad M_j''=\pm1,\quad M_j'=\pm1,\quad M_j''=\pm2,0,$$

$$M_j'=\pm0,\quad M_j''=\pm1. \quad (22a)$$

From the form of I_+ the following selection rules are found:

$$M_j'''=2,\quad M_j=1,\quad M_j'''=1,\quad M_j=0,\quad M_j'''=0,$$

$$M_j=-1,\quad M_j'''=-1,\quad M_j=-2 \quad (22b)$$

for a total of 24 combinations. The conditions for echo maximum amplitude are determined by the intramolecular interactions which cause the relative spin phases to become refocussed at time $t=\tau$ after the second pulse, resulting in the formation of the principal echo. This condition imposes a further restriction on Eq. (22), namely $M_j'''^2-M_j^2=-(M_j''^2-M_j'^2)$, thus reducing the number of selection rules to the following eight combinations:

$$M_j=1,\quad M_j'=\pm 2,\quad M_j''=\pm 1,\quad M_j'''=2,$$

$$M_j=0,\quad M_j'=\pm 1,\quad M_j''=0,\quad M_j'''=1,$$

$$M_j=-1,\quad M_j'=0,\quad M_j''=\pm 1,\quad M_j'''=0,$$

$$M_j=-2,\quad M_j'=\pm 1,\quad M_j''=\pm 2,\quad M_j'''=-1, \tag{23a}$$

for each of which

$$M_k=M_k''',\quad M_k'=M_k''. \tag{23b}$$

Considering the relevant matrix elements, for $I=1$ we arrive at the same result obtained by Yu *et al.*[8]

$$M_j=0,\quad M_j'=\pm 1,\quad M_j''=0,\quad M_j'''=1,$$

$$M_j=-1,\quad M_j'=0,\quad M_j''=\pm 1,\quad M_j'''=0. \tag{24}$$

Computation of Eq. (21) yields expressions for the principal echo amplitude of the form

$$S(I=1)=\frac{5}{6}(1-X)[a+b\cos(\overline{\delta_{12}}\tau)+c\cos(2\overline{\delta_{12}}\tau)+d\cos(3\overline{\delta_{12}}\tau)+e\cos(4\overline{\delta_{12}}\tau)]+X[l+m\cos(\overline{\delta_{11}}\tau)+n\cos(2\overline{\delta_{11}}\tau)], \tag{25a}$$

$$S(I=2)=\frac{5}{6}(1-X)[A+B\cos(\overline{\delta_{22}}\tau)+C\cos(2\overline{\delta_{22}}\tau)+D\cos(3\overline{\delta_{22}}\tau)+E\cos(4\overline{\delta_{22}}\tau)]+X[L+M\cos(\overline{\delta_{21}}\tau)+N\cos(2\overline{\delta_{21}}\tau)]. \tag{25b}$$

The coefficients $A,B,\ldots,N,a,b,\ldots,n$ are functions of the pulse parameters $\underline{\beta}$ and φ and the inhomogeneous field represented by $\cos(2\underline{\alpha_j}\tau)$ and are presented explicitly in the Appendix. Note that for $X=1$ (no $I=2$ spins), Eq. (25a) reduces to Eq. (12a) reported by Yu *et al.*[8] which applies to H_2, except for a $\pi/2$ phase shift reflecting the difference in conventions used for the definition of the pulse terms. Assuming that the inhomogeneous field is independent of the intermolecular dipole interactions, for $\beta=\pi/2$, Eq. (25) reduces to a form in which the influence of the inhomogeneous field is more obvious,

$$S_{xx}=-P(1-\cos(2\alpha_j\tau)),$$

$$S_{xy}=P(1+\cos(2\alpha_j\tau)), \tag{26a}$$

in which case P is a function independent of the pulse parameters

$$P(I=1)=\frac{5}{6}(1-X)\left(\frac{7}{8}+\cos(\overline{\delta_{12}}\tau)+2\cos(2\overline{\delta_{12}}\tau)+\cos(3\overline{\delta_{12}}\tau)+\frac{1}{8}\cos(4\overline{\delta_{12}}\tau)\right)+X\left(\frac{1}{2}+2\cos(\overline{\delta_{11}}\tau)+\frac{1}{2}\cos(2\overline{\delta_{11}}\tau)\right), \tag{26b}$$

$$P(I=2)=\frac{5}{6}(1-X)\left(\frac{7}{8}+\cos(\overline{\delta_{22}}\tau)+2\cos(2\overline{\delta_{22}}\tau)+\cos(3\overline{\delta_{22}}\tau)+\frac{1}{8}\cos(4\overline{\delta_{22}}\tau)\right)+X\left(\frac{1}{2}+2\cos(\overline{\delta_{21}}\tau)+\frac{1}{2}\cos(2\overline{\delta_{21}}\tau)\right). \tag{26c}$$

This interpretation represents a significant departure from the development used for the analysis of p-H_2 (Ref. 8) where, in the absence of unlike $I\neq 0$ spins, the dipolar field is entirely described by the two terms $\cos(\overline{\delta_{11}}\tau)$ and $\cos(2\overline{\delta_{11}}\tau)$. Moreover, both these terms and the one arising from the inhomogeneous field were taken as averages over the sample [$\overline{\cos(2\alpha\tau)}=(1/N)\Sigma_j\cos(2\overline{\alpha_j}\tau)$, for example] and used as arbitrary parameters to fit the data obtained for each set of experimental conditions. Assumed to be relevant for the p-D_2 fraction in solid deuterium, the previous development[10] also neglected the dipolar interactions between unlike spins, i.e., the tacit assumption that $\overline{\delta_{12}}=0$ was made. Despite these shortcomings, two useful relations were discovered that remain valid. From Eq. (26) a measure of the inhomogeneous field is obtained by forming the ratio

$$\mathcal{R}=\frac{|S_{xx}+S_{xy}|}{|S_{xx}|+|S_{xy}|}=\cos(2\overline{\alpha_j}\tau). \tag{27}$$

Also, information of the spin-spin relaxation due to the dipolar field can be extracted by combining the results for an xx and xy sequence for a given set of experimental parameters

$$|S_{xx}|+|S_{xy}|=P. \tag{28}$$

Confirmation of the validity of Eqs. (27) and (28) by comparison to the experimental results will at once verify both the independence of the inhomogeneous field on the dipolar interactions and the detailed form of the echo amplitude decay from dipolar relaxation arrived at in Eq. (25).

III. RESULTS AND DISCUSSION

A. Echo amplitudes and decay: the anomalous p-D_2 behavior

One of the most intriguing and as yet unexplained phenomena found in solid D_2 is the striking departure from Curie's law for the $I=1$ magnetization with decreasing temperature.[6,10] This deviation is particularly strong for $X=0.5$ and in the temperature range where the orientational fluctuation rate τ_Q^{-1} is of the same order as the Larmor frequency ω_L of the processing spins.[19] This departure from Curie's law means an apparent ''loss'' of spins in the sample and various scenarios have been proposed in an unsuccessful attempt to explain this phenomenon. No such ''loss'' is observed for the $I=2$ spins in the same sample, nor for the $I=1$ spins in solid H_2 at comparable mole fractions X and at temperatures where $\omega_L\tau_Q\approx 1$.[19] Therefore, in solid D_2, the amplitude ratio $S_{xy}(I=1)/S_{xy}(I=2)$ in the limit $\tau\to 0$ is smaller than the calculated ratio of the nuclear susceptibilities and is a function of T and X.

For the observable p-D_2 $I=1$ spins, the solid echo decay is affected by the orientational fluctuations in the tempera-

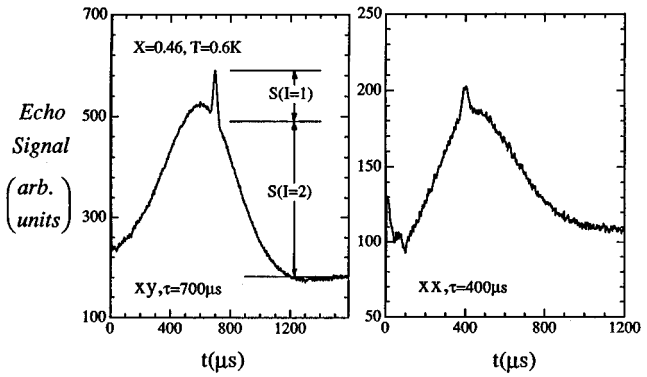

FIG. 1. Representative echo profiles for the *xy* and *xx* pulse sequences and the absolute amplitudes $S(I=1)$ and $S(I=2)$ of the principal echo, in arbitrary units, as taken from Ref. 10.

ture region where $\omega_L \tau_Q \approx 1$ and the theory of the enhanced echo damping caused by these fluctuations has been presented by Harris *et al.*[19] In our analysis of the echo relaxation data, for simplicity we have only considered samples studied under conditions where this fluctuational damping is small. For instance, we do not attempt to account for the behavior of samples with $X=0.49$ at temperatures below $T=0.4$ K where orientational fluctuations are considerable. The magnitude of this damping and the damping characteristic temperature decrease with X. Hence samples with $X=0.28$ at $T=0.2$ K will show only small fluctuation damping[19] and will be analyzed as described below.

We point out that there is no correlation between the observed solid echo magnitudes of the different samples shown in the various figures, since the settings of the electronics are not necessarily kept the same for different experiments, as they were chosen to optimize the recording conditions.

B. Echo amplitude relaxation

Our computations are compared with tabulated experimental data of Ref. 10. Representative echo profiles for the *xy* and *xx* pulse sequences are shown in Fig. 1. The absolute value of each in the same arbitrary units is reproduced here, but the amplitude is positive relative to the free induction decay for the *xy* and negative for the *xx* echoes. The signal amplitudes, $S(I=1)$ and $S(I=2)$, for *para* and *ortho*-D_2 respectively, are also defined. For $I=1$, the signal maximum of the principal echo is located at a time $t=\tau$ after the second pulse, as expected. The asymmetry of the broader $I=2$ echo envelope and the apparent shift of the echo maximum amplitude are due to intermolecular dipole relaxation and have been interpreted in terms of a Gaussian line shape centred at a time $t=\tau$ after the second pulse and damped by an exponential decay.[10,20] From measurements of the inhomogeneous and intermolecular second moments, the typical values found are $\overline{\alpha_j}=150$ Hz and $\overline{\delta_{jk}}=220$ Hz for the mean dipolar field[10] for both *para* and *ortho*-D_2. [There is a small relative frequency shift $\delta\overline{\alpha_j}$, (Ref. 20) between *para* and *ortho*-D_2 but it does not affect the individual analyses of $S(I=1)$ and $S(I=2)$.]

Figure 2 shows the representative echo amplitude decay of a sample with $X=0.49$ at 0.6 K and $X=0.45$ at 0.4 K as a function of the evolution time τ for both the *xx* and *xy* sequences with $\beta=\pi/2$. With increasing values of τ the echo

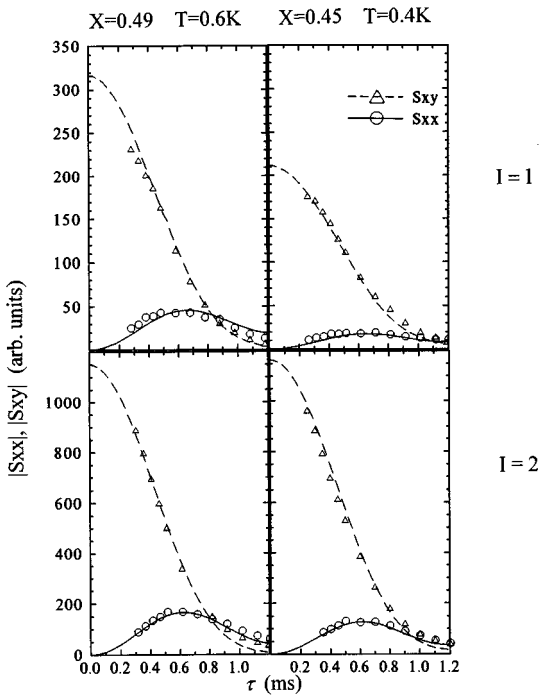

FIG. 2. Echo amplitude decay of the absolute amplitudes $S(I=1)$ and $S(I=2)$ for a sample with $X=0.49$ at 0.6 K and $X=0.45$ at 0.4 K as a function of the evolution time τ for both the *xy* (triangles) and *xx* (circles) pulse sequences with $\beta=90°$. For each sample, the arbitrary units are the same. The symbols represent the experimental data while the broken and solid curves are the computed decays using the coupling constants reported in Table I and described in the text.

amplitudes are damped through both the intermolecular dipole and inhomogeneous fields. The relevant parameters are determined by simultaneous fit of the theory to the data from the *xx* and *xy* sequences, with the lines representing the best fits of Eq. (26). Table I gives a summary of the parameters used to produce relaxation curves similar to those in Fig. 2 for various samples over a range of conditions, from which a few trends are immediately apparent. (These parameters can be varied individually to within about 5% without deterioration of the fit and are comparable with the experimentally observed values reported in Ref. 10 from a simpler analysis.) They are consistent in the sense that it is expected that both the *ortho* and *para* fractions are subject to the same inhomogeneous broadening and hold for both the respective *xx* and *xy* sequences. There is no well established trend in the magnitude of this inhomogeneous field with X. At $\beta=\pi/2$, the amplitude of the S_{xx} signal is small relative to S_{xy} resulting in unfavorable S/N and large experimental scatter. While this problem is not as significant for the $I=2$ signal, the error is amplified when the data are processed via Eqs. (27) and (28). A survey of Table I also suggests that our understanding of the dipolar relaxation is adequate in that $\delta_{11} \approx \delta_{21}$ and $\delta_{12} \approx \delta_{22}$.

In Fig. 3 the fit of the combined Eqs. (26) and (28) is given for the same set of experimental data used in Fig. 2. Here the theoretical curves are independent of the inhomogeneous field and show the dependence of the signal amplitude on the intermolecular dipole relaxation alone. The theoretical results for the four-parameter (solid line) and two-

TABLE I. Summary of the theoretical coupling constants used throughout the analysis. Note that the $X=0.45$ sample at 0.1 K (marked by the asterisk) is affected by the additional damping from orientational fluctuations, as described in the text, resulting in larger than expected values for $\overline{\delta_{11}}$ and $\overline{\delta_{12}}$. The observed trend in the magnitudes of the dipolar coupling constants is as expected for the different values of X, i.e., $\overline{\delta_{j1}}$ increases and $\overline{\delta_{j2}}$ decreases as X increases. While samples with larger X tend to exhibit larger values of α_j, there is no reason to expect a correlation between these two quantities.

X	T (K)	$\overline{\alpha(I=1)}$ (Hz)	$\overline{\delta_{11}}$ (Hz)	$\overline{\delta_{12}}$ (Hz)	$\overline{\alpha(I=2)}$ (Hz)	$\overline{\delta_{21}}$ (Hz)	$\overline{\delta_{22}}$ (Hz)
0.06	0.1				120		223
0.06	0.2				120		223
0.06	1.2				120		223
0.28	0.2	125	64	175	120	64	191
0.30	1.2	92	107	199	104	127	203
0.40	0.6	95	107	199	107	111	207
0.45*	0.1	123	130	195	123	115	215
0.45	0.4	115	111	191	123	127	199
0.45	1.0	115	111	191	123	115	199
0.49	0.6	145	119	187	155	135	195

parameter (broken line) representations of the dipolar field are compared using the values reported in Table I. Making the assumption that Eq. (7) holds and using average values of the relevant coupling constants yields the broken curve for the two-parameter model. This last fit to the experimental data deviates from them somewhat more than the less restrictive four-parameter fit. However, these theoretical results do support the notion that the dipolar field experienced by all spins in the sample can be effectively represented by two distinct contributions given by $\overline{\delta_{j1}}$ and $\overline{\delta_{j2}}$. It is also significant that these dipolar coupling terms reveal a more sensitive dependence of the signal amplitudes on the presence of the *ortho* spins than on the *para* fraction, which is not surprising when one considers the difference in spin magnitudes but perhaps this also hints at the distribution of environments experienced by the o-D_2 molecules.

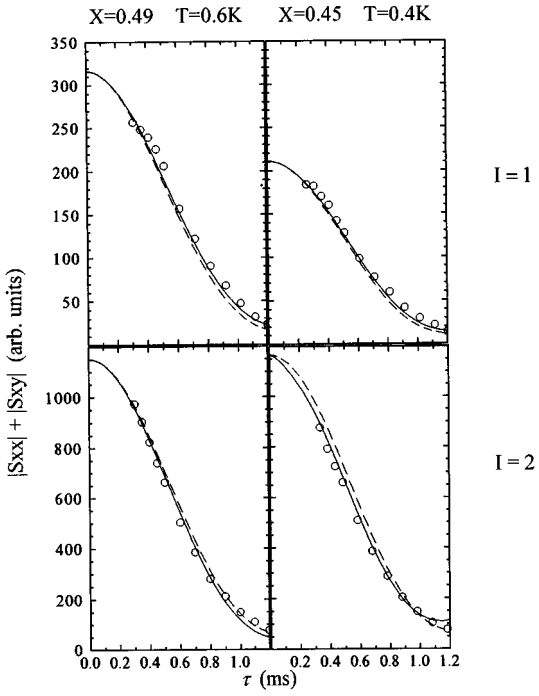

FIG. 3. Fit of Eq. (28) to the same set of experimental data used in Fig. 2. The theoretical curves are independent of the inhomogeneous field and show the dependence of the signal amplitude decay on the intermolecular dipole relaxation alone. The results of both the two-parameter and four-parameter representations of the dipolar field are given. The solid curves result from the coupling constants reported in Table I. The broken curves are the result of the two-parameter fit assuming $\overline{\delta_{21}}=\overline{\delta_{11}}$ and $\overline{\delta_{22}}=\overline{\delta_{12}}$ using average values.

The data from these two samples were again used to produce Fig. 4. The data (open circles) are compared with the curves calculated from Eq. (27) where the values of the inhomogeneous field $\overline{\alpha_j}$ in Table I have been used. The experimental scatter is exacerbated in this case owing to the fact that the difference in phase of S_{xx} and S_{xy} leads to a subtraction. This operation cancels out the effect of the intermolecular dipole interaction, yet despite this more serious deviation of the theory it is noted that the inhomogeneous field appears to be uncoupled from the intermolecular dipolar field. Again it is apparent that the inhomogeneous field affects each spin in the sample in a uniform fashion and has only a slightly larger effect on the sample with the larger concentration of $I=1$ spins. While our basic understanding of the $\overline{\delta_{jk}}$'s is good, the origin of the inhomogeneous field is unclear as discussed previously.[10]

In Fig. 5, for a sample with $X=0.28$ and $T=0.2$ K (incorrectly labeled $X=0.24$ in Fig. 7 of Ref. 10), the dependence of the signal amplitude on the angle of the second pulse, β, is presented for four different values of τ. This set of experiments represents the most demanding examination of the validity of the entire theoretical model, as it incorporates systematic variations of all experimentally significant parameters. The values of the parameters reported in Table I are the averages of those used to fit all four sets of data and were varied within 10% in order to closely match the experimental points. The increasing deviations from these means generally arise from results with larger values of τ. As pre-

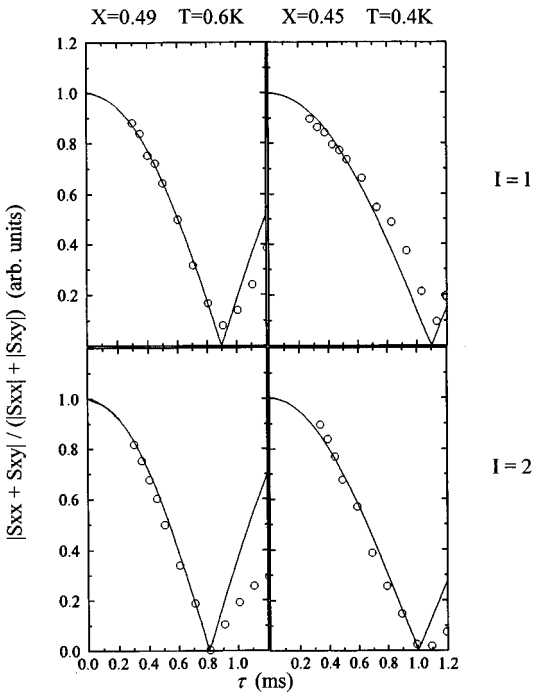

FIG. 4. Fit of Eq. (27) to the experimental data for samples with $X=0.49$ at $T=0.6$ K and $X=0.45$ at 0.4 K. The theoretical curve shows the contribution of the inhomogeneous field alone to the signal amplitude decay and its independence on the dipolar field. Fit parameters used are reported in Table I.

viously discussed, given the form of $\overline{\delta_{jk}}$ expressed in Eq. (6), it is tacitly expected that for a spin j coupled to the field generated by surrounding spins $I_k=1$, $\overline{\delta_{j1}}$ should decrease with decreasing X, a trend observed from the results for Figs. 2, 3, and 5 shown in Table I. While the reverse should be true for $I_k=2$, i.e., $\overline{\delta_{j2}}$ should increase with decreasing X, the results suggest more efficient coupling to spins $I_k=2$ in lattices with larger concentrations of $I=1$ molecules. Despite this apparent contradiction in the expected behavior of the dipolar field, we do note that the average values of $\overline{\delta_{j1}}$ and $\overline{\delta_{j2}}$ appear to be independent of the magnitude of the spin j, hence $\overline{\delta_{21}}\approx\overline{\delta_{11}}$ and $\overline{\delta_{22}}\approx\overline{\delta_{12}}$ consistently throughout this analysis as expected. The fit of the theory to the experimental data presented in Fig. 5 makes use of the four-parameter procedure because here an attempt is made to simultaneously account for the influence of all relevant parameters. There is increasing disparity between the theoretical curves and the experimental evidence for large values of both τ and β, the common cause being the dephasing of the prepared coherences. Apart from the unfavorable S/N typical for low amplitude signals, as the amplitudes decrease with increasing τ and β the effects of imperfect pulse tuning become increasingly important and thus some systematic deviation might be introduced. This heralds the breakdown of the two-parameter model for the dipolar field, as increasingly divergent values of the $\overline{\delta_{jk}}$'s must be used in order to closely match the experimental data for the longer values of τ. However, a relaxation mechanism hitherto unaccounted for may exist. Spin diffusion and the motion of neighboring atoms or defects should have negligible influences at these temperatures, but

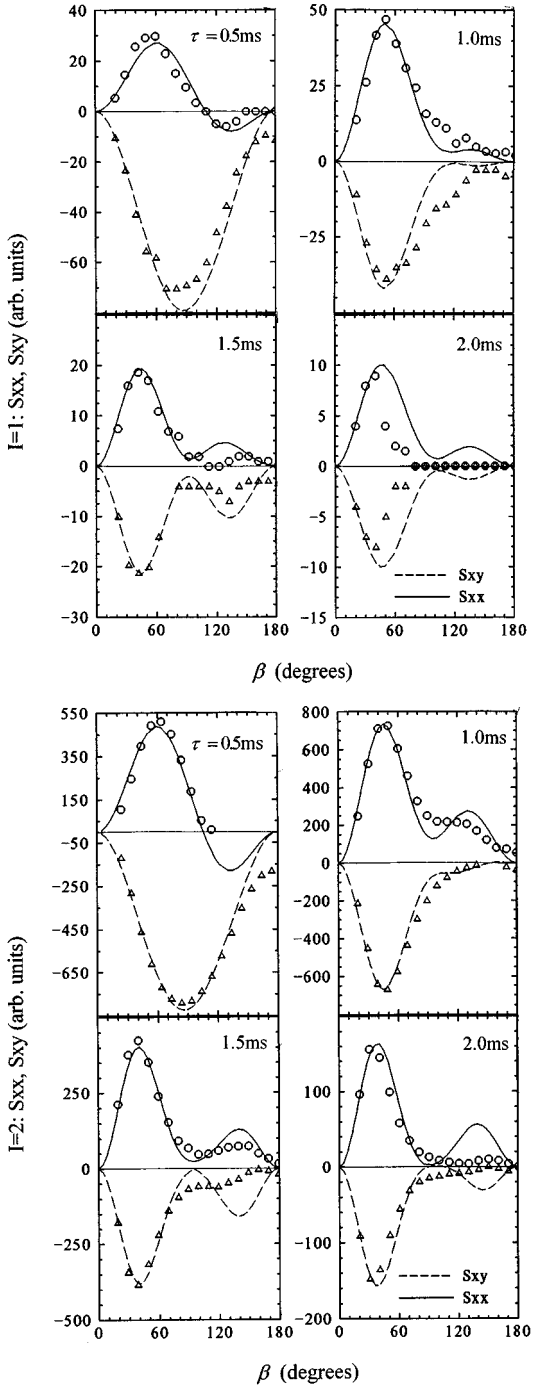

FIG. 5. Dependence of the signal amplitude on the angle of the second pulse, β, for four different values of τ for a sample with $X=0.28$ at $T=0.2$ K. The symbols (circles for S_{xx}, triangles for S_{xy}) mark the experimental data and the solid and broken curves, the best fit of the theory. For $I=1$ the fit parameters for all four sets of data are $\overline{\alpha_j}=120$ Hz, $\overline{\delta_{11}}=64$ Hz, $\overline{\delta_{12}}=175$ Hz. For $I=2$: $\overline{\alpha_j}=120$ Hz, $\overline{\delta_{22}}=190$ Hz, $\overline{\delta_{21}}=64$ Hz. The values of the dipole coupling terms were varied individually to within 10%, with increasing deviation at large values of τ.

it remains possible for cross relaxation to be effective. This would manifest itself as a zero-quantum ($\Delta M=0$) exchange of polarization between two spins and might have been neglected due to the strictly secular representation of the intermolecular dipolar interaction.

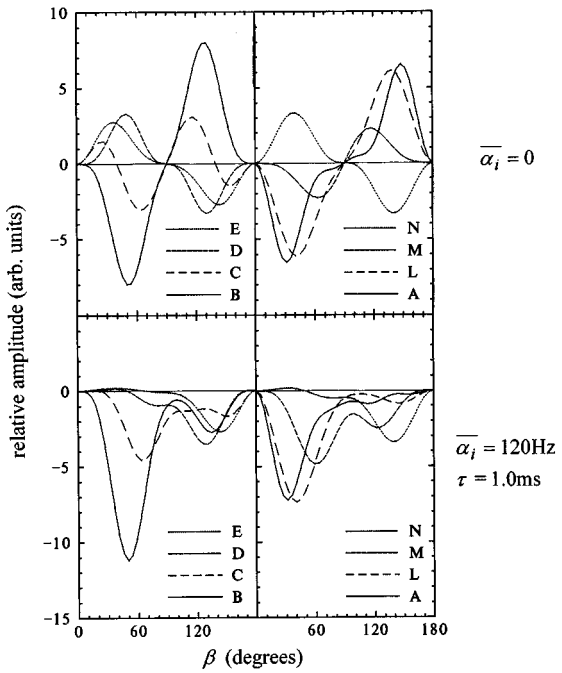

FIG. 6. Individual amplitudes of the parameters defined in Eq. (25b) and listed in the Appendix, used for the theoretical curves in Fig. 5 for the $I=2$, S_{xx} signal amplitudes. Top for $\overline{\alpha_j}=0$ and bottom for $\overline{\alpha_j}=120$ Hz and $\tau=1.0$ ms.

For the $I=2$ S_{xx} case, Fig. 6 shows how these theoretical curves are constituted of the functions $A,B,\ldots,N$ defined by Eq. (25) and presented in the Appendix. In the absence of an inhomogeneous field, these functions are dependent only upon the pulse terms and have odd symmetry about $\beta=\pi/2$. However, when $\overline{\alpha_j}\neq 0$, those contributions associated with the higher frequency dipole terms (E and N for example) are favored at larger values of β, as shown in Fig. 6 where $\overline{\alpha_j}=120$ Hz and $\tau=1.0$ ms. It should be expected, then, that such high frequency terms are attenuated for increasing values of τ, as evidenced in Fig. 5.

C. Positions of principal and satellite echoes

In order to account for the positions of the principal and satellite echoes for $I=2$, the frequencies of the relevant coherences must be determined. To summarize, the eigenvalues of the molecular states of total spin I are calculated by considering the intramolecular quadrupole and dipolar energies of the atomic spin states. Table II shows how these molecular states are constructed and presents the corresponding eigenvalues under the Hamiltonian of Eq. (2). Note that the states $|x\rangle$ and $|y\rangle$ are linear combinations of the *ortho* $I=0$ and $I=2$, $M=0$ states which are mixed through elements in the flip-flop terms of the intramolecular dipole contribution. Assuming that the splitting $6a_j-b_j$ between the $|x\rangle$ and $|y\rangle$ states is large relative to the intermolecular nuclear dipole interaction (recall $\overline{\delta_{jk}}\approx 100$ Hz), the latter is treated as a nondegenerate first order perturbation as these states can be considered to be uncoupled. Table III shows the frequencies of the single quantum coherences $|M\rangle\langle M'|$ from which four transitions in the frequency domain are expected, namely,

TABLE II. Energies of the molecular states for o-D_2.

Molecular state $\lvert M_i\rangle$	Eigenvalue
$\lvert 2\rangle=\lvert 11\rangle$	$-2\overline{\alpha_j}+2a_j+b_j+2\sum_{k\neq j}\overline{\delta_{jk}}I_{zk}$
$\lvert 1\rangle=(1/\sqrt{2})[\lvert 10\rangle+\lvert 01\rangle]$	$-\overline{\alpha_j}-a_j-b_j/2+\sum_{k\neq j}\overline{\delta_{jk}}I_{zk}$
$\lvert x\rangle=(1/\sqrt{2})[\lvert -11\rangle+\lvert 1-1\rangle]$	$2a_j-b_j$
$\lvert y\rangle=\lvert 00\rangle$	$-4a_j$
$\lvert -1\rangle=(1/\sqrt{2})[\lvert -10\rangle+\lvert 0-1\rangle]$	$\overline{\alpha_j}-a_j-b_j/2-\sum_{k\neq j}\overline{\delta_{jk}}I_{zk}$
$\lvert -2\rangle=\lvert -1-1\rangle$	$2\overline{\alpha_j}+2a_j+b_j-2\sum_{k\neq j}\overline{\delta_{jk}}I_{zk}$

$$\nu-\nu_0=\pm\left(3a_j+\frac{3b_j}{2}\right)=\pm X_1$$

and

$$\nu-\nu_0=\pm\left(3a_j-\frac{b_j}{2}\right)=\pm X_2. \tag{29}$$

During the first time interval τ, the spins accumulate a phase $\pm 2\pi X_n\tau$ relative to the Larmor frequency that can be refocussed subsequent to the second pulse, which has the effect of mixing these coherences. Formation of the principal echo is due to those two components that do not change relative phase, subject to the condition $X_n t=X_n\tau$, while two satellite echoes are possible, corresponding to the two coherence changes $X_1 t=X_2\tau$ and $X_2 t=X_1\tau$. Using the frequencies of these $\Delta M=\pm 1$ transitions, echoes are expected to be found at $t=k\tau$ where $k=X_1/X_2$, 1, X_2/X_1 or

$$k=\frac{t}{\tau}=\frac{1+3b_j/2a_j}{1-b_j/2a_j},\quad 1,\quad \frac{1-b_j/2a_j}{1+3b_j/2a_j}, \tag{30}$$

which is equivalent to the expression obtained by Volz *et al.*[12] and Conradi *et al.*[21] for $a=3a_j$, where a different convention for the nuclear quadrupole interaction is used. Note from Eq. (6) that while a_j and b_j are functions of the polarization and the relative orientation of the molecular axis and the external magnetic field, the ratios appearing in Eq. (30) are not. It would be expected, therefore, that the values of k would be independent of the orientational ordering, the

TABLE III. Frequencies of the single quantum operators for o-D_2.

Operator $\lvert M\rangle\langle M'\rvert$	Frequency
$\lvert 2\rangle\langle 1\rvert$	$-\overline{\alpha_j}+3a_j+3b_j/2+\sum_{k\neq j}\overline{\delta_{jk}}I_{zk}$
$\lvert 1\rangle\langle x\rvert$	$-\overline{\alpha_j}-3a_j+b_j/2+\sum_{k\neq j}\overline{\delta_{jk}}I_{zk}$
$\lvert 1\rangle\langle y\rvert$	$-\overline{\alpha_j}+3a_j-b_j/2+\sum_{k\neq j}\overline{\delta_{jk}}I_{zk}$
$\lvert x\rangle\langle -1\rvert$	$-\overline{\alpha_j}+3a_j-b_j/2+\sum_{k\neq j}\overline{\delta_{jk}}I_{zk}$
$\lvert y\rangle\langle -1\rvert$	$-\overline{\alpha_j}-3a_j+b_j/2+\sum_{k\neq j}\overline{\delta_{jk}}I_{zk}$
$\lvert -1\rangle\langle -2\rvert$	$-\overline{\alpha_j}-3a_j-3b_j/2+\sum_{k\neq j}\overline{\delta_{jk}}I_{zk}$

mole fraction of $I=1$ spins and the admixture between the $J=0$ and $J=2$ rotational states and would be given by $k=0.845$, 1, and 1.183. This exemplifies the fact that I is not a good quantum number for o-D_2, otherwise we would expect Solomon echoes at $k=1/3$, 1, and 3.[22]

Whether or not the satellite echoes are observed, however, will depend upon the admixture of the rotational states for in the spherically symmetrical $J=0$ state the values of a_j and b_j both vanish and the frequencies of Table II collapse to a single degenerate transition. Even given finite values of these coupling terms it is necessary that the broadened NMR lines represented in Eq. (28) are well resolved. The $k\neq l$ satellite echoes described in Ref. 12 for HD and o-D_2 embedded in an amorphous silica substrate, a system with large crystal fields, are not observed in solid D_2 (see Fig. 8 of Ref. 10). Use of the values $a_j=290$ Hz and $b_j=-70$ Hz [obtained from Eq. (5) for $C_{\mathrm{SR}}(X,T)=0.02$ and $(1-3\cos^2\theta_{H,zj})=1$, corresponding to a weakly oriented system[23]] in Eq. (29) shows that the frequency separation $|X_1|-|X_2|$ is only about 150 Hz, which is comparable to the inhomogeneous broadening frequency $\overline{\alpha_j}=130$ Hz. Given this situation, it is likely that the satellites are not observed because of the weak orientational ordering of the o-D_2 fraction. The weak polarization indicated by the admixture coefficient $C_{\mathrm{SR}}(X,T)$ results in the small observed values of the intramolecular coupling constants a_j and b_j. Consequently, the frequencies of the single quantum coherences shown in Table III become degenerate and only the $k=1$ echoes may form. In contrast, the crystal field must have been very large for the experiments on D_2 embedded in an amorphous silicon matrix.[12] There, the strength of the orientational ordering is already evident from the sharpness of the principal echo, indicating significant NMR line broadening. Under these conditions, $C_{\mathrm{SR}}(X,T)$ may well be of the order of unity and therefore $|X_1|-|X_2|$ will be much larger than any small local field inhomogeneity resulting in observable satellite echoes.

IV. SUMMARY

We have presented a formal theory for the solid echo amplitude of both the *ortho* and *para* fractions in solid D_2. The numerical results obtained for the contributions to the spin-pair dipolar field and the inhomogeneous magnetic field are consistent with those obtained from analysis of the experimental line shapes: observed signal amplitude decay is well approximated in terms of our model for dipolar spin relaxation and inhomogeneous line broadening. Similarly, the experimentally observed dependence upon the parameters of the pulse sequence is accounted for as well, in terms of the evolution of the detailed dipole-dipole coupling terms. The magnitude of these terms is consistent with expectations, however, the origin of the inhomogeneous field needs clarification.

While the satellite echoes expected for the $I=2$ fraction of solid D_2 have not been observed, we posit that it is a combination of weak crystal fields and the existence of inhomogeneous broadening that contribute to the lack of resolution of the NMR frequency spectrum, resulting in quenching of the satellites.

The inhomogeneous field as well as the possible existence of unaccounted relaxation mechanisms need further discussion. Given this development of a more comprehensive theory for the response of the solid deuteriums to two pulse NMR experiments, it is hoped that further interest in these concerns will be generated.

ACKNOWLEDGMENTS

The financial support of the National Sciences and Engineering Research of Canada (NSERC) and McGill University is gratefully recognized. T.R.J.D. would like to thank the Walter Sumner Foundation for financial support. One of the authors (H.M.) acknowledges a helpful discussion with A. B. Harris. The authors are indebted to D. Clarkson for his help with solid echo data retrieval and representation.

APPENDIX: EXPLICIT FORMULATION OF THE FUNCTIONS DEFINED IN EQ. (25) OF THE TEXT

Evaluation of Eq. (21) subject to the selection rules of Eqs. (22)–(24) was performed with the help of MAPLE to derive Eq. (25). The MAPLE code also contains a routine for the evaluation of the general form of the rotation matrices of Eq. (12). Listed below are the terms required to reproduce the theoretical results. The MAPLE source code will be made available to interested parties who send a request by e-mail, addressed to one of the authors (T.R.J.D. or B.C.S.).

$$a:\quad (1+2\cos^2\beta\,\cos^2\varphi-2\cos^2\varphi-\cos^2\beta)\left(\frac{35}{8}\cos^4\beta+\frac{5}{2}\cos^3\beta-\frac{9}{4}\cos^2\beta-\frac{1}{2}\cos\beta+\frac{7}{8}\right)$$

$$+(1-\cos^2\beta)\cos(2\overline{\alpha_j}\tau)\left(\frac{35}{8}\cos^4\beta-\frac{5}{2}\cos^3\beta-\frac{9}{4}\cos^2\beta+\frac{1}{2}\cos\beta+\frac{7}{8}\right),$$

$$b:\quad (1+2\cos^2\beta\,\cos^2\varphi-2\cos^2\varphi-\cos^2\beta)(-7\cos^4\beta-2\cos^3\beta+6\cos^2\beta+2\cos\beta+1)$$

$$+(1-\cos^2\beta)\cos(2\overline{\alpha_j}\tau)(-7\cos^4\beta+2\cos^3\beta+6\cos^2\beta-2\cos\beta+1),$$

$$c: \quad (1+2\cos^2\beta\,\cos^2\varphi-2\cos^2\varphi-\cos^2\beta)\left(\frac{7}{2}\cos^4\beta-2\cos^3\beta-\frac{9}{2}\cos^2\beta+\cos\beta+2\right)$$

$$+(1-\cos^2\beta)\cos(2\overline{\alpha_j}\tau)\left(\frac{7}{2}\cos^4\beta+2\cos^3\beta-\frac{9}{2}\cos^2\beta-\cos\beta+2\right),$$

$$d: \quad (1+2\cos^2\beta\cos^2\varphi-2\cos^2\varphi-\cos^2\beta)(-\cos^4\beta+2\cos^3\beta-2\cos\beta+1)$$

$$+(1-\cos^2\beta)\cos(2\overline{\alpha_j}\tau)(-\cos^4\beta-2\cos^3\beta+2\cos\beta+1),$$

$$e: \quad (1+2\cos^2\beta\,\cos\,\varphi-2\cos^2\varphi-\cos^2\beta)\left(\frac{1}{8}\cos^4\beta-\frac{1}{2}\cos^3\beta+\frac{3}{4}\cos^2\beta-\frac{1}{2}\cos\beta+\frac{1}{8}\right)$$

$$+(1-\cos^2\beta)\cos(2\overline{\alpha_j}\tau)\left(\frac{1}{8}\cos^4\beta+\frac{1}{2}\cos^3\beta+\frac{3}{4}\cos^2\beta+\frac{1}{2}\cos\beta+\frac{1}{8}\right),$$

$$l: \quad (1+2\cos^2\beta\,\cos^2\varphi-2\cos^2\varphi-\cos^2\beta)\left(\frac{3}{2}\cos^2\beta+\cos\beta+\frac{1}{2}\right)+(1-\cos^2\beta)\cos(2\overline{\alpha_j}\tau)\left(\frac{3}{2}\cos^2\beta-\cos\beta+\frac{1}{2}\right),$$

$$m: \quad (1+2\cos^2\beta\,\cos^2\varphi-2\cos^2\varphi-\cos^2\beta)(2-2\cos^2\beta)+2(1-\cos^2\beta)^2\cos(2\overline{\alpha_j}\tau),$$

$$n: \quad (1+2\cos^2\beta\,\cos^2\varphi-2\cos^2\varphi-\cos^2\beta)\left(\frac{1}{2}\cos^2\beta-\cos\beta+\frac{1}{2}\right)+(1-\cos^2\beta)\cos(2\overline{\alpha_j}\tau)\left(\frac{1}{2}\cos^2\beta+\cos\beta+\frac{1}{2}\right),$$

$$A: \quad \left(\frac{35}{4}\cos^4\beta+5\cos^3\beta-\frac{9}{2}\cos^2\beta-\cos\beta+\frac{7}{4}\right)\Big(\cos^2\varphi\,\cos^4\beta-\frac{1}{2}\cos^4\beta+2\cos^2\varphi\,\cos^3\beta-\cos^3\beta-2\cos^2\varphi\,\cos\beta+\cos\beta$$

$$-\cos^2\varphi+\frac{1}{2}+18\cos^2\beta(2\cos^2\varphi\,\cos^2\beta-\cos^2\beta-2\cos^2\varphi+1)\Big)+\cos(2\overline{\alpha_j}\tau)\Big(\frac{35}{8}\cos^4\beta-\frac{5}{2}\cos^3\beta$$

$$-\frac{9}{4}\cos^2\beta+\frac{1}{2}\cos\beta+\frac{7}{8}\Big)(1-2\cos\beta+2\cos^3\beta-\cos^4\beta-9(\cos^2\beta-1)\cos^2\beta),$$

$$B: \quad (-7\cos^4\beta-2\cos^3\beta+6\cos^2\beta+2\cos\beta+1)\Big(\cos^2\varphi\,\cos^4\beta-\frac{1}{2}\cos^4\beta+2\cos^2\varphi\,\cos^3\beta-\cos^3\beta-2\cos^2\varphi\,\cos\beta$$

$$+\cos\beta-\cos^2\varphi+\frac{1}{2}+9\cos^2\beta(2\cos^2\varphi\,\cos^2\beta-\cos^2\beta-2\cos^2\varphi+1)\Big)+\cos(2\overline{\alpha_j}\tau)(-7\cos^4\beta+2\cos^3\beta$$

$$+6\cos^2\beta-2\cos\beta+1)(1-2\cos\beta+2\cos^3\beta-\cos^4\beta-9(\cos^2\beta-1)\cos^2\beta),$$

$$C: \quad \left(\frac{7}{2}\cos^4\beta+2\cos^3\beta-\frac{9}{2}\cos^2\beta-\cos\beta+2\right)(2\cos^2\varphi\,\cos^4\beta-\cos^4\beta+4\cos^2\varphi\,\cos^3\beta-2\cos^3\beta-4\cos^2\varphi\,\cos\beta$$

$$+2\cos\beta-2\cos^2\varphi+1+9\cos^2\beta(2\cos^2\varphi\,\cos^2\beta-\cos^2\beta-2\cos^2\varphi+1))+\cos(2\overline{\alpha_j}\tau)\Big(\frac{7}{2}\cos^4\beta-2\cos^3\beta$$

$$-\frac{9}{2}\cos^2\beta+\cos\beta+2)(1-2\cos\beta+2\cos^3\beta-\cos^4\beta-9(\cos^2\beta-1)\cos^2\beta),$$

$$D: \quad (-\cos^4\beta+2\cos^3\beta-2\cos\beta+1)(2\cos^2\varphi\,\cos^4\beta-\cos^4\beta+4\cos^2\varphi\,\cos^3\beta-2\cos^3\beta-4\cos^2\varphi\,\cos\beta+2\cos\beta$$

$$-2\cos^2\varphi+1+9\cos^2\beta(2\cos^2\varphi\,\cos^2\beta-\cos^2\beta-2\cos^2\varphi+1))+\cos(2\overline{\alpha_j}\tau)(-\cos^4\beta-2\cos^3\beta$$

$$+2\cos\beta+1)(1-2\cos\beta+2\cos^3\beta-\cos^4\beta-9(\cos^2\beta-1)\cos^2\beta),$$

$$E:\quad \left(\frac{1}{8}\cos^4\beta-\frac{1}{2}\cos^3\beta+\frac{3}{4}\cos^2\beta-\frac{1}{2}\cos\beta+\frac{1}{8}\right)(2\cos^2\varphi\,\cos^4\beta-\cos^4\beta+4\cos^2\varphi\,\cos^3\beta-2\cos^3\beta$$
$$-4\cos^2\varphi\,\cos\beta+2\cos\beta-2\cos^2\varphi+1+9\cos^2\beta(2\cos^2\varphi\,\cos^2\beta-\cos^2\beta-2\cos^2\varphi+1))$$
$$+\cos(2\overline{\alpha_j}\tau)\left(\frac{1}{8}\cos^4\beta+\frac{1}{2}\cos^3\beta+\frac{3}{4}\cos^2\beta+\frac{1}{4}\cos\beta+\frac{1}{8}\right)(1-2\cos\beta+2\cos^3\beta$$
$$-\cos^4\beta-9(\cos^2\beta-1)\cos^2\beta),$$

$$L:\quad \left(\frac{3}{2}\cos^2\beta+\cos\beta+\frac{1}{2}\right)(2\cos^2\varphi\,\cos^4\beta-\cos^4\beta+4\cos^2\varphi\,\cos^3\beta-2\cos^3\beta-4\cos^2\varphi\,\cos\beta+2\cos\beta-2\cos^2\varphi$$
$$+1+9\cos^2\beta(2\cos^2\varphi\,\cos^2\beta-\cos^2\beta-2\cos^2\varphi+1))+\cos(2\overline{\alpha_j}\tau)\left(\frac{3}{2}\cos^2\beta-\cos\beta+\frac{1}{2}\right)(1-2\cos\beta$$
$$+2\cos^3\beta-\cos^4\beta-9(\cos^2\beta-1)\cos^2\beta),$$

$$M:\quad (2-2\cos\beta)(2\cos^2\varphi\,\cos^4\beta-\cos^4\beta+4\cos^2\varphi\,\cos^3\beta-2\cos^3\beta-4\cos^2\varphi\,\cos\beta+2\cos\beta-2\cos^2\varphi+1$$
$$+18\cos^2\beta(2\cos^2\varphi\,\cos^2\beta-\cos^2\beta-2\cos^2\varphi+1))+\cos(2\overline{\alpha_j}\tau)(1-\cos\beta)(2-4\cos\beta+4\cos^3\beta$$
$$-2\cos^4\beta-18(\cos^2\beta-1)\cos^2\beta),$$

$$N:\quad \left(\frac{1}{2}-\cos\beta+\frac{1}{2}\cos^2\beta\right)(2\cos^2\varphi\,\cos^4\beta-\cos^4\beta+4\cos^2\varphi\,\cos^3\beta-2\cos^3\beta-4\cos^2\varphi\,\cos\beta+2\cos\beta-2\cos^2\varphi$$
$$+1+9\cos^2\beta(2\cos^2\varphi\,\cos^2\beta-\cos^2\beta-2\cos^2\varphi+1))+\cos(2\overline{\alpha_j}\tau)\left(\frac{1}{2}+\cos\beta+\frac{1}{2}\cos^2\beta\right)(1-2\cos\beta$$
$$+2\cos^3\beta-\cos^4\beta-9(\cos^2\beta-1)\cos^2\beta).$$

*Electronic address: dinesen@omc.lan.mcgill.ca
†Electronic address: bryans@omc.lan.mcgill.ca

[1] I. F. Silvera, Rev. Mod. Phys. **52**, 393 (1980).
[2] A. B. Harris and H. Meyer, Can. J. Phys. **63**, 3 (1985).
[3] N. S. Sullivan, C. M. Edwards, Y. Lin, and D. Zhou, Can. J. Phys. **65**, 1463 (1987).
[4] J. Van Kranendonk, *Solid Hydrogen* (Plenum, New York, 1983).
[5] A. B. Harris, S. Washburn, and H. Meyer, J. Low Temp. Phys. **50**, 152 (1983); S. Washburn and H. Meyer, J. Low Temp. Phys. **57**, 31 (1984) on H_2 and references therein.
[6] M. Calkins, R. Banke, X. Li, and H. Meyer, J. Low Temp. Phys. **65**, 47 (1986); **65**, 90 (1986) on D_2 and references therein.
[7] A. B. Harris, Phys. Rev. B **2**, 3495 (1970).
[8] I. Yu, S. Washburn, and H. Meyer, J. Low Temp. Phys. **51**, 369 (1983).
[9] I. Yu, S. Washburn, M. Calkins, and H. Meyer, J. Low Temp. Phys. **51**, 401 (1983).
[10] D. Clarkson, X. Qin, and H. Meyer, J. Low Temp. Phys. **91**, 119 (1993).
[11] X. Qin, D. Clarkson, and H. Meyer, J. Low Temp. Phys. **91**, 153 (1993).
[12] M. P. Volz, P. Santos-Filho, M. S. Conradi, P. A. Fedders, and R. E. Norberg, Phys. Rev. Lett. **63**, 2582 (1989).
[13] N. F. Ramsey, *Molecular Beams* (Oxford, London, 1956).
[14] A. Abragam, *The Principles of Nuclear Magnetism* (Clarendon, Oxford, 1961).
[15] A. B. Harris (private communication).
[16] N. S. Sullivan, M. Devoret, B. P. Cowan, and C. Urbina, Phys. Rev. B **17**, 5016 (1978).
[17] S. Lacelle and L. Tremblay, J. Chem. Phys. **102**, 947 (1995); D. A. Drabold and P. A. Fedders, Phys. Rev. A **135**, 715 (1988).
[18] A. R. Edmonds, *Angular Momentum in Quantum Mechanics*, 3rd ed. (Princeton University, Princeton, NJ, 1974).
[19] A. B. Harris, H. Meyer, and X. Qin, Phys. Rev. B **49**, 3844 (1994).
[20] X. Qin and H. Meyer, Phys. Rev. B **49**, 3857 (1994).
[21] M. S. Conradi, P. A. Fedders, and R. E. Norberg, in *Pulsed Magnetic Resonance, A Recognition of E. L. Hahn*, edited by D. M. S. Bagguley (Clarendon, Oxford, 1992), p. 238.
[22] I. Solomon, Phys. Rev. **110**, 61 (1958).
[23] R. Banke, X. Li, D. Clarkson, and H. Meyer, J. Low Temp. Phys. **72**, 99 (1988).